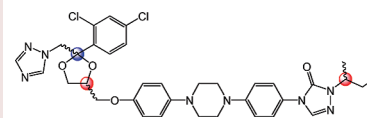


Impact of Absolute Stereochemistry on the
Antiangiogenic and Antifungal Activities of ItraconazoleWei Shi,[†] Benjamin A. Nacev,^{†,§} Shridhar Bhat,[†] and Jun O. Liu^{*,†,‡}[†]Department of Pharmacology and Molecular Sciences, [‡]Department of Oncology, and [§]Medical Scientist Training Program, Johns Hopkins School of Medicine, 725 North Wolfe Street, Baltimore, Maryland 21205

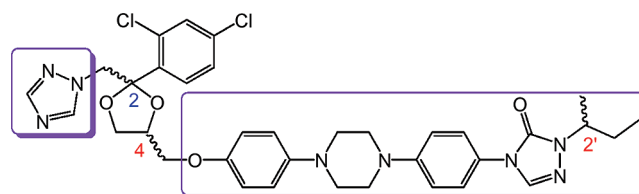
ABSTRACT Itraconazole is used clinically as an antifungal agent and has recently been shown to possess antiangiogenic activity. Itraconazole has three chiral centers that give rise to eight stereoisomers. The complete role of stereochemistry in the two activities of itraconazole, however, has not been addressed adequately. For the first time, all eight stereoisomers of itraconazole (**1a–h**) have been synthesized and evaluated for activity against human endothelial cell proliferation and for antifungal activity against five fungal strains. Distinct antiangiogenic and antifungal activity profiles of the *trans* stereoisomers, especially **1e** and **1f**, suggest different molecular mechanisms underlying the antiangiogenic and antifungal activities of itraconazole.

KEYWORDS Itraconazole, stereochemistry, diastereomers, angiogenesis, antifungal activity



We have previously reported that itraconazole (Figure 1), an antifungal drug, potently inhibits *in vitro* proliferation of human umbilical vein endothelial cells (HUVEC) and angiogenesis *in vivo*.¹ The target responsible for itraconazole's antifungal activity is lanosterol 14 α -demethylase (14DM), a key enzyme involved in the biosynthesis of ergosterol, which is required for the integrity of the fungal cell membrane.² However, the role of human 14DM in the inhibition of angiogenesis by itraconazole remains unclear. The poor correlation between human 14DM inhibition and antiangiogenic activity for several structurally related potent azole antifungal drugs implies that an other primary molecular target(s) might be responsible for the antiangiogenic activity of itraconazole with 14DM making only a partial contribution.^{1,3,4}

Itraconazole contains three chiral centers, giving rise to a total of eight stereoisomers. The dioxolane ring harbors two chiral centers, while the third one marked as 2' resides on the *sec*-butyl side chain appended to the triazolone ring (Figure 1). As an antifungal drug, itraconazole is administered in clinical formulations as a 1:1:1:1 mixture of four *cis*-stereoisomers (**1a–d**).⁵ Although the antifungal activity⁶ and metabolism⁵ of individual *cis* stereoisomers of itraconazole have been reported, the activity of the *trans* stereoisomers, **1e–h**, have not been disclosed to date. Furthermore, itraconazole has not been examined for antiangiogenic activity in any of its stereochemically pure forms. Our previous effort was limited to the synthesis and determination of the antiangiogenic activity of the epimeric mixtures of 4*R*- and 4*S*-*cis*-itraconazole.¹ To systematically explore the effect of absolute stereochemistry at every chiral center of itraconazole on both antifungal and antiangiogenic activity,



1a	<i>cis</i> -2 <i>S</i> ,4 <i>R</i> ,2' <i>S</i>	1e	<i>trans</i> -2 <i>S</i> ,4 <i>S</i> ,2' <i>S</i>
1b	<i>cis</i> -2 <i>S</i> ,4 <i>R</i> ,2' <i>R</i>	1f	<i>trans</i> -2 <i>S</i> ,4 <i>S</i> ,2' <i>R</i>
1c	<i>cis</i> -2 <i>R</i> ,4 <i>S</i> ,2' <i>S</i>	1g	<i>trans</i> -2 <i>R</i> ,4 <i>R</i> ,2' <i>S</i>
1d	<i>cis</i> -2 <i>R</i> ,4 <i>S</i> ,2' <i>R</i>	1h	<i>trans</i> -2 <i>R</i> ,4 <i>R</i> ,2' <i>R</i>

Figure 1. Structures of the eight itraconazole diastereomers arising from three stereogenic centers numbered 2, 4, and 2'. The *cis* designation denotes that the two substituents (in the blue boxes) are on the same side of the 1,3-dioxolane ring, while the *trans* designation denotes the opposite orientation.

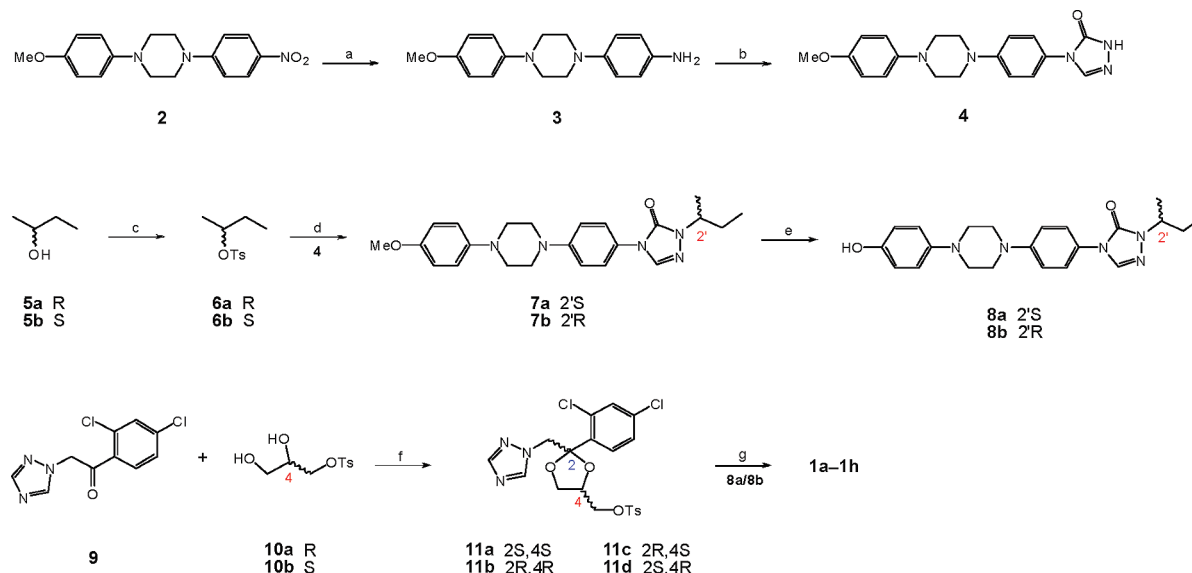
we synthesized all of the eight stereoisomers and compared their antiangiogenic and antifungal activities.

We began the total synthesis by reducing the nitro group in *N*-(4-methoxyphenyl)-*N'*-(4-nitrophenyl)-piperazine **2** (Scheme 1)¹ using a palladium-catalyzed transfer hydrogenation. Instead of ammonium formate that we had used in our earlier synthesis, the use of hydrazine as a hydrogen source⁷ produced much higher yields of aniline **3**. Palladium-catalyzed reduction of the nitro group to the amino group was achieved in a better yield than our earlier synthesis using ammonium formate as a hydrogen

Received Date: January 10, 2010

Accepted Date: March 29, 2010

Published on Web Date: April 12, 2010

Scheme 1. Synthesis of Eight Itraconazole Stereoisomers^a

^a Reagents and conditions: (a) 10% Pd/C, $\text{NH}_2\text{NH}_2 \cdot \text{H}_2\text{O}$, EtOH, reflux, 99%. (b) (i) Phenyl chloroformate, pyridine, CH_3CN ; (ii) $\text{NH}_2\text{NH}_2 \cdot \text{H}_2\text{O}$, 1,4-dioxane, reflux; (iii) formamidine acetate, AcOH, DMF, 80 °C, 81% over 3 steps. (c) TsCl, Et_3N , DMAP, CH_2Cl_2 , 99%. (d) K_2CO_3 , 18-Crown-6, DMSO, room temperature, 73%. (e) 48% Aqueous HBr, 110 °C, 91%. (f) TFOH, toluene, room temperature, 60 h, 63% for *cis* and 19% for *trans* based on NMR. (g) NaH, DMSO, 50 °C \rightarrow 85 °C, 62%.

source.¹ Without further purification, the amino group in **3** was transformed into the triazolone via the phenylcarbamate and semicarbazide intermediates.⁸ A small amount of acetic acid was added to facilitate the cyclization of the semicarbazide with formamidine acetate at a lower temperature than usual for this type of ring closure, thereby minimizing side reactions.⁹ The stereochemistry at the 2' position in **1a–h** was inherited from the optically pure starting material, (*R*)-(-)-2-butanol (**5a**) or (*S*)-(+)-2-butanol (**5b**). The chiral tosylate **6a** or **6b** was obtained in almost quantitative yield by reacting **5a** or **5b** with tosyl chloride in the presence of triethylamine and DMAP. To achieve a stereospecific *N*-alkylation of triazolone **4** by tosylate displacement of **6a** or **6b**, the proton abstraction of triazolone nitrogen was conducted using potassium carbonate in conjunction with 18-crown-6. Such an application of crown ethers is known to enhance the nucleophilicity of the nitrogen anion by forming loose ion pairs.¹⁰ In addition to driving the reaction to proceed at room temperature, this avoided a potential $\text{S}_{\text{N}}1$ reaction as well as minimized the elimination reaction of **6a** or **6b**. A clean $\text{S}_{\text{N}}2$ inversion leading to either **7a** or **7b** in an enantiomerically pure form has been documented before.^{11,12} The desired stereochemical outcome at this step in our synthesis was also confirmed later by chiral high-performance liquid chromatography (HPLC) analysis of **1a** and **1b** (Table 1 and the Supporting Information). Removal of the methyl group by heating **7a** or **7b** in concentrated aqueous HBr at 110 °C yielded **8a** or **8b** containing a free phenol ready for the final coupling.⁸

Construction of the 1,3-dioxolane ring in **11a–d** was achieved by acid-assisted ketalization of 2,2',4'-trichloroace-

Table 1. Chiral HPLC Analysis Data and Optical Rotation of Itraconazole Stereoisomers

compounds	retention time (min) ^a	diastereomeric purity	$[\alpha]_{\text{D}}$ in CHCl_3
<i>cis</i>	1a (2 <i>S</i> ,4 <i>R</i> ,2' <i>S</i>)	43.017	-5.5
	1d (2 <i>R</i> ,4 <i>S</i> ,2' <i>R</i>)	42.520	+5.7
	1b (2 <i>S</i> ,4 <i>R</i> ,2' <i>R</i>)	46.333	-12.3
	1c (2 <i>R</i> ,4 <i>S</i> ,2' <i>S</i>)	42.547	+12.6
<i>trans</i>	1e (2 <i>S</i> ,4 <i>S</i> ,2' <i>S</i>)	38.933	-13.2
	1h (2 <i>R</i> ,4 <i>R</i> ,2' <i>R</i>)	39.573	+13.3
	1f (2 <i>S</i> ,4 <i>S</i> ,2' <i>R</i>)	37.800	-19.1
	1g (2 <i>R</i> ,4 <i>R</i> ,2' <i>S</i>)	39.253	+18.6

^a HPLC conditions are almost identical to those in ref 5.

tophenone **9** with optically pure glyceryl tosylate **10a** or **10b**.¹⁰ While the stereochemistry at C-4 in **11a–d** emanates from the chiral starting material **10a** or **10b**, C-2 is the new chiral center that gets created during ketalization and therefore numbered in blue. The ratio of *cis* versus *trans* diastereomers **11a/11c** or **11b/11d** is dictated by the steric effects, and actually, a preponderance of *cis*-dioxolane was observed. The *cis* diastereomer (**11a** or **11b**)¹³ was separated from the *trans* diastereomer (**11c** or **11d**) and further purified by the well-established double recrystallization approach.¹⁰ To date, however, among the *trans* diastereomers, only **11c** could be traced in the literature to a fleeting citation, and surprisingly, **11d** is unknown. After a meticulous thin-layer chromatographic analysis, it was found that the tosylate salts of the *trans* diastereomer predominantly remained in the ethyl acetate solution during the purification process of the *cis* product. By running a gradient column (50:1 \rightarrow 5:1 CH_2Cl_2 -acetone), **11c** was isolated from **11a** and other side products with purity that was sufficient for NMR characterization.

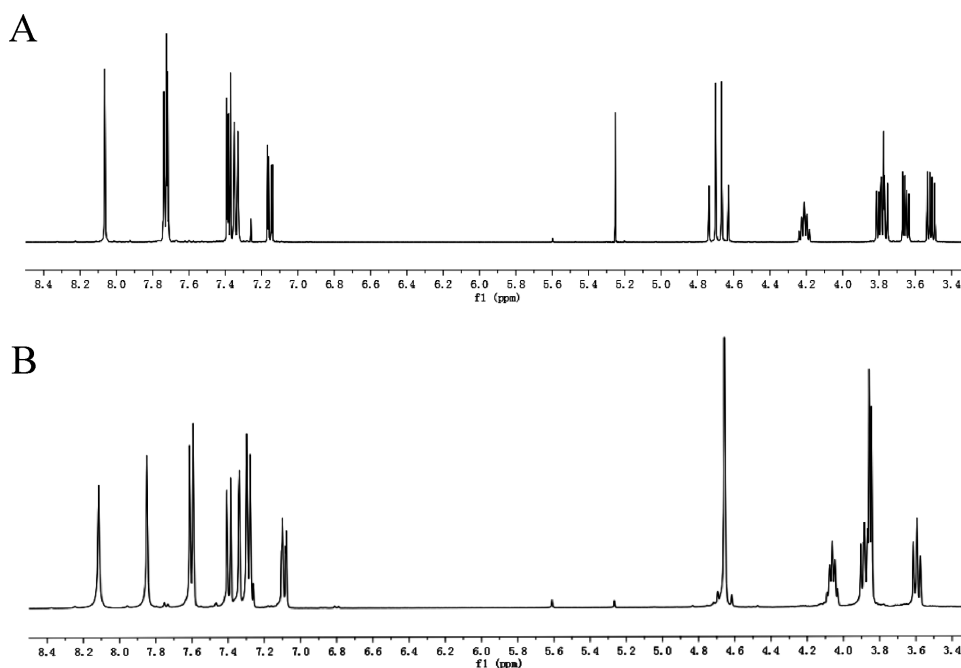


Figure 2. ^1H and ^{13}C NMR of 1,3-dioxolane intermediates **11a–d**. (A) ^1H NMR for *cis*-**11a** and **11b**. (B) ^1H NMR for *trans*-**11c** and **11d**.

Table 2. Potency of Itraconazole Stereoisomers in Biological Assays

compounds	HUVEC		<i>Saccharomyces cerevisiae</i> (BY4741)		<i>C. albicans</i> (10261)		<i>C. neoformans</i> (H99)		<i>Candida glabrata</i>			
	IC ₅₀ ^a	R ^b	MIC ₈₀ ^c	R ^b	MIC ₈₀ ^c	R ^b	MIC ₈₀ ^c	R ^b	BG1		B92	
									MIC ₈₀ ^c	R ^b	MIC ₈₀ ^c	R ^b
racemic itraconazole ^d	93 (76, 115.3)	1	0.5	1	0.0156	1	0.0625	1	0.5	1	0.5	1
1a (2 <i>S</i> ,4 <i>R</i> ,2' <i>S</i>)	74 (62, 115)	0.8	2	4	0.0312	2	0.125	2	0.5	1	0.5	1
1b (2 <i>S</i> ,4 <i>R</i> ,2' <i>R</i>)	106 (82, 138)	1.1	1	2	0.0156	1	0.25	4	0.5	1	0.5	1
1c (2 <i>R</i> ,4 <i>S</i> ,2' <i>S</i>)	147 (123, 177)	1.6	2	4	0.0312	2	0.125	2	0.5	1	0.5	1
1d (2 <i>R</i> ,4 <i>S</i> ,2' <i>R</i>)	236 (183, 305)	2.5	1	2	0.0312	2	0.25	4	0.5	1	0.5	1
1e (2 <i>S</i> ,4 <i>S</i> ,2' <i>S</i>)	289 (212, 393)	3.1	1	2	0.0312	2	4	64	1	2	1	2
1f (2 <i>S</i> ,4 <i>S</i> ,2' <i>R</i>)	361 (181, 719)	3.9	1	2	0.0156	1	4	64	0.5	1	0.5	1
1g (2 <i>R</i> ,4 <i>R</i> ,2' <i>S</i>)	301 (173, 525)	3.2	>4	>8	0.5	32	1	16	>4	>8	>4	>8
1h (2 <i>R</i> ,4 <i>R</i> ,2' <i>R</i>)	346 (236, 508)	3.7	>4	>8	0.5	32	2	32	>4	>8	>4	>8

^a nM (95% CI). ^b Ratios of IC₅₀ or MIC₈₀ of stereoisomer/racemic mixture. ^c μg/mL. ^d Mixture of the four *cis*-diastereomers from Sigma-Aldrich.

Similarly, pure **11d** was also obtained. The ^1H NMR spectra (Figure 2A,B) illustrate the obvious differences not only in the aromatic region (7.0–8.5 ppm) but also in the aliphatic region (3.4–4.8 ppm), arising from different 1,3-dioxolane ring conformations in the *cis* and *trans* diastereomers.

With the building blocks in hand, the displacement of the *O*-tosyl group in **11a–d** with the phenolic oxygen in **8a,b** under basic conditions afforded final products **1a–h**.⁸ Because the chiral centers on the 1,3-dioxolane ring are well separated from the third chiral center on the *sec*-butyl side chain, it is not surprising that the *cis* diastereomers could be well distinguished from the *trans* diastereomers by NMR, whereas all of the *cis* stereoisomers **1a–d** or the *trans* stereoisomers **1e–h** exhibited identical ^1H and ^{13}C NMR

spectra. To provide further support for the successful synthesis and purification of all eight stereoisomers, the optical rotation and chiral HPLC profile of each stereoisomer was measured (Table 1 and Supporting Information).

After the quality of all stereoisomers was confirmed, the potency of each stereoisomer against HUVEC proliferation and fungal growth was determined (Table 2). HUVEC were incubated with drug or vehicle alone for 24 h and then pulsed for 6 h with [^3H]-thymidine, the incorporation of which was taken as a readout of cell proliferation. Inhibition of fungal growth was assayed by incubating five yeast strains with 2-fold serial dilutions of each stereoisomer for 30–60 h depending on the strain (see the methods in the Supporting Information) and then measuring the OD₆₀₀ of the

culture to quantitate growth. The minimum concentration capable of inhibiting growth by 80% (MIC_{80}) was determined.

The influence of stereochemistry on the inhibition of HUVEC proliferation by itraconazole was minor. The difference in potency between **1a** and **1f**, the most and least potent stereoisomers, respectively, was only slightly greater than 4-fold. The most relevant stereochemical determinant of potency in HUVEC was the configuration of the dioxolane ring, with the *cis* diastereomers exhibiting higher potency than the *trans* series by several fold. We note that the *cis*-4*R* diastereomer is slightly more potent than the *cis*-4*S* isomer. This is contrary to our previous report.¹ After carefully examining the individual steps of the previous synthesis, it appears that the stereochemical centers were misassigned. Hence, we also wish to redress our earlier account with the stereochemical assignments and the corresponding assay data in this letter. In contrast to HUVEC, the potency of itraconazole against fungal proliferation was highly influenced by stereochemistry (Table 2). We observed a difference in potency of up to 32-fold between stereoisomers in one fungal strain. In four out of five strains tested, the least potent stereoisomers by a margin of at least 4–32-fold were two of the *trans* isomers, **1g** and **1h**. On the other hand, the other *trans* pair **1e** and **1f** was about as potent as the *cis* diastereomers (**1a–d**). The exception was *Cryptococcus neoformans* in which **1e** and **1f** were 2-fold less potent than **1g** and **1h** and 32-fold less potent than the best inhibitor.

In the case of dioxolane-containing azole antifungals like itraconazole, ketoconazole, and terconazole, it has been noted long ago that the *cis* diastereomeric pairs exhibit much higher antifungal potency over their *trans* counterparts, and thus, for efficacy reasons, they have been used clinically as mixtures of *cis* diastereomers. Docking studies performed based on the published fluconazole-MtCYP51 (referred to as 14DM for the human enzyme) crystal structure have offered an explanation to this effect.¹⁴ Rupp et al. analyzed homology-modeled CaCYP51 complexed with different stereoisomers of ketoconazole.¹⁵ Interestingly, they concluded that the *cis* pair (2*S*,4*R* and 2*R*,4*S*) and only one of the *trans* pair, namely, 2*S*,4*S*-ketoconazole, avidly bind to CaCYP51, which is in good agreement with the reported IC_{50} values of the stereoisomers of ketoconazole against *Candida albicans*.¹⁶ Antifungal activities that we measured for the eight stereoisomers of itraconazole against the three ascomycetes perfectly match the pattern observed with ketoconazole. It is possible that the CYP51 enzymes of ascomycetes poorly bind the 2*R*,4*R*-itraconazole, whereas in the case of phylogenetically distant *C. neoformans*, this scenario of binding among the *trans* pairs is quite the opposite. This may also be explained by the expression of a stereoselective efflux pump or catabolic enzyme in this strain. Taken together, these data indicate that unlike HUVEC inhibition, the sensitivity of fungal growth to itraconazole is dictated not by *cis–trans* configuration of the dioxolane ring but instead by the absolute stereochemistry at the 2 and 4 carbons. The only commonality that we observed for the role of stereochemistry in HUVEC and fungal inhibition was that the stereochemistry at the 2' position had little influence on potency in either case.

In summary, all of the *cis* diastereomers that make up the commercial itraconazole exhibited high potency in both HUVEC and fungal inhibition. All of the *trans* diastereoisomers were less potent in HUVEC proliferation than were the *cis* diastereoisomers. In contrast, one pair of *trans* diastereoisomers, **1e** and **1f**, was roughly as potent as the *cis* diastereomers with respect to antifungal activity against four out of five strains. The lack of correlation between HUVEC and fungal sensitivity to optically pure itraconazole stereoisomers suggests that human 14DM is not likely to be the major target for the antiangiogenic activity of itraconazole. Indeed, we have recently found that the inhibitory effect of itraconazole on endothelial cells results largely from its inhibition of cholesterol trafficking through the lysosomal compartment, leading to inhibition of the mTOR pathway.¹⁷ This work provides previously unavailable data on the role of stereochemistry in the potency of itraconazole against an emerging therapeutic target for this drug, angiogenesis. We demonstrated that compounds **1a** and **1b** possess the greatest antiangiogenic potential and should therefore be used as lead compounds for further optimization of itraconazole as an antiangiogenic drug.

SUPPORTING INFORMATION AVAILABLE Experimental procedure, analytical data, and ¹H and ¹³C NMR spectra for new compounds **11c,d** and **1e–h**. HRMS and HPLC data for final compounds **1a–h**. This material is available free of charge via the Internet at <http://pubs.acs.org>.

AUTHOR INFORMATION

Corresponding Author: *To whom correspondence should be addressed. E-mail: joliu@jhu.edu.

Funding Sources: This work was supported by NCI, FAMRI, the Commonwealth Foundation, and the NIH Medical Scientist Training Program Grant T32GM07309 (B.A.N.). It was also supported in part by Grant UL1 RR 025005 from the National Center for Research Resources (NCRR), a component of the National Institutes of Health (NIH) and NIH Roadmap for Medical Research, and its contents are solely the responsibility of the authors and do not necessarily represent the official view of NCRR or NIH.

ACKNOWLEDGMENT We are grateful to Drs. Peter Espen-shade and Brendan Cormack and Clara Bien for providing us with the fungal strains and for helpful advice on conducting the fungal growth assays. We also thank Professor Gerald Hart for the use of equipment.

REFERENCES

- (1) Chong, C. R.; Xu, J.; Lu, J.; Bhat, S.; Sullivan, D. J., Jr.; Liu, J. O. Inhibition of Angiogenesis by the Antifungal Drug Itraconazole. *ACS Chem. Biol.* **2007**, *2*, 263–270.
- (2) Vanden Bossche, H.; Marichal, P.; Gorrens, J.; Coene, M. C. Biochemical basis for the activity and selectivity of oral antifungal drugs. *Br. J. Clin. Pract. Suppl.* **1990**, *71*, 41–46.
- (3) David, C. L.; Diane, E. K.; Michael, R. W.; Maria, S.; Damjana, R.; Steven, L. K. Characteristics of the heterologously expressed

- human lanosterol 14 α -demethylase (other names: P45014DM, CYP51, P45051) and inhibition of the purified human and *Candida albicans* CYP51 with azole antifungal agents. *Yeast* **1999**, *15*, 755–763.
- (4) Trösken, E. R.; Michael Arand, M. A.; Zarn, J. A.; Patten, C.; Völkel, W.; Lutz, W. K. Comparison of lanosterol-14 α -demethylase (CYP51) of human and *Candida albicans* for inhibition by different antifungal azoles. *Toxicology* **2006**, *228*, 24–32.
- (5) Kunze, K. L.; Nelson, W. L.; Kharasch, E. D.; Thummel, K. E.; Isoherranen, N. Stereochemical aspects of itraconazole metabolism in vitro and in vivo. *Drug Metab. Dispos.* **2006**, *34*, 583–590.
- (6) Koch, P.; Rossi, R. F., Jr.; Senanayake, C. H.; Wald, S. A. 2R,4S-Hydroxyitraconazole isomers. WO 00/66100, 2000.
- (7) Höglund, L. P. J.; Silver, S.; Engström, M. T.; Salo, H.; Tauber, A.; Kyyrönen, H.-K.; Saarenketo, P.; Hoffrén, A.-M.; Kokko, K.; Pohjanoksa, K.; Sallinen, J.; Savola, J.-M.; Wurster, S.; Kallatsa, O. A Structure-Activity Relationship of Quinoline Derivatives as Potent and Selective α_2C -Adrenoceptor Antagonists. *J. Med. Chem.* **2006**, *49*, 6351–6363.
- (8) Heeres, J.; Backx, L. J. J.; Cutsem, J. V. Antimycotic Azoles. 7. Synthesis and Antifungal Properties of a Series of Novel Triazol-3-ones. *J. Med. Chem.* **1984**, *27*, 894–900.
- (9) Sheng, C.; Zhang, W.; Ji, H.; Zhang, M.; Song, Y.; Xu, H.; Zhu, J.; Miao, Z.; Jiang, Q.; Yao, J.; Zhou, Y.; Zhu, J.; Lü, J. Structure-Based Optimization of Azole Antifungal Agents by CoMFA, CoMSIA, and Molecular Docking. *J. Med. Chem.* **2006**, *49*, 2512–2515.
- (10) Tanoury, G. J.; Hett, R.; Wilkinson, H. S.; Wald, S. A.; Senanayake, C. H. Total synthesis of (2R,4S,2'S,3'R)-hydroxyitraconazole: Implementations of a recycle protocol and a mild and safe phase-transfer reagent for preparation of the key chiral units. *Tetrahedron: Asymmetry* **2003**, *14*, 3487–3493.
- (11) Tanoury, G. J.; Senanayake, C. H.; Hett, R.; Kuhn, A. M.; Kessler, D. W.; Wald, S. A. Pd-Catalyzed Aminations of Aryl Triazoines: Effective Synthesis of Hydroxyitraconazole Enantiomers. *Tetrahedron Lett.* **1998**, *39*, 6845–6848.
- (12) Pinori, M. L. M.; Modena, D.; Mascagni, P. Azole Derivative Useful as Antifungal Agents with Reduced Interaction with Metabolic Cytochromes. WO 2005040156, 2005.
- (13) *cis*- and *trans*-Designations describe the geometrical relationship of triazolylmethyl (C-2) and oxymethyl (C-4) substituents, either on the same face (*cis*) or the opposite face (*trans*) of the dioxolane ring. While going from tosyl derivatives (**11a–d**) all the way to itraconazole stereoisomers **1a–h**, the *cis* and *trans* relationship does not change. However, according to Cahn–Ingold–Prelog priority rules, the *R* and *S* notations corresponding to C-4 of the dioxolane ring do change. For example, *cis*-2S,4S tosylate derivative (**11a**) eventually leads to *cis*-2S,4R,2'S (**1a**) or *cis*-2S,4R,2'R (**1b**) itraconazole stereoisomers.
- (14) Podust, L. M.; Poulos, T. L.; Waterman, M. R. Crystal structure of cytochrome P450 14 α -sterol demethylase (CYP51) from *Mycobacterium tuberculosis* in complex with azole inhibitors. *Proc. Nat. Acad. Sci.* **2001**, *98*, 3068–3073.
- (15) Rupp, B.; Raub, S.; Marian, C.; Holtje, H.-D. Molecular design of two sterol 14 α -demethylase homology models and their interactions with the azole antifungals ketoconazole and bifonazole. *J. Comput.-Aided Mol. Des.* **2005**, *19*, 149–163.
- (16) Rotstein, D. M.; Kertesz, D. J.; Walker, K. A.; Swinney, D. C. Stereoisomers of ketoconazole: Preparation and biological activity. *J. Med. Chem.* **1992**, *35*, 2818–2825.
- (17) Xu, J.; Dang, Y.; Ren, R. Y.; Liu, J. O. Cholesterol trafficking is required for mTOR activation in endothelial cells. *Proc. Natl. Acad. Sci. U.S.A.* **2010**, *107*, 4764–4769.